Marine Pollution Bulletin 174 (2022) 113194

Contents lists available at ScienceDirect

Marine Pollution Bulletin

journal homepage: www.elsevier.com/locate/marpolbul

Integrating remote sensing methods during controlled exposure experiments to quantify group responses of dolphins to navy sonar☆

J.W. Durban [a,b,*], B.L. Southall [a,c], J. Calambokidis [d], C. Casey [a,c], H. Fearnbach [e], T.W. Joyce [f], J. A. Fahlbusch [d,g], M.G. Oudejans [h], S. Fregosi [a], A.S. Friedlaender [a,c], N.M. Kellar [b], F. Visser [h,i,j]

[a] Southall Environmental Associates, Inc., 9099 Soquel Drive, Aptos, CA 95003, USA
[b] Marine Mammal and Turtle Division, Southwest Fisheries Science Center, National Marine Fisheries Service, 8901 La Jolla Shores Drive, La Jolla, CA 92037, USA
[c] Institute of Marine Sciences, University of California Santa Cruz, 115 McAllister Way, Santa Cruz, CA 95060, USA
[d] Cascadia Research Collective, 218 1/2 W 4th Ave., Olympia, WA 98501, USA
[e] SR3 SeaLife Response, Rehabilitation and Research, 2003 S. 216th St. #98811, Des Moines, WA 98198, USA
[f] Environmental Assessment Services, 350 Hills St., Suite 112, Richland, WA 99354, USA
[g] Department of Biology, Hopkins Marine Station, Stanford University, Pacific Grove, CA 93950, USA
[h] Kelp Marine Research, 1624 CJ Hoorn, the Netherlands
[i] Department of Freshwater and Marine Ecology, Institute for Biodiversity and Ecosystem Dynamics, University of Amsterdam, P.O. Box 94240, 1090 GE Amsterdam, the Netherlands
[j] Department of Coastal Systems, Royal Netherlands Institute for Sea Research, P.O. Box 59, 1790 AB Den Burg, Texel, the Netherlands

ARTICLE INFO

Keywords:
Cetacean
Common dolphin
Noise
Behaviour

ABSTRACT

Human noise can be harmful to sound-centric marine mammals. Significant research has focused on characterizing behavioral responses of protected cetacean species to navy mid-frequency active sonar (MFAS). Controlled exposure experiments (CEE) using animal-borne tags have proved valuable, but smaller dolphins are not amenable to tagging and groups of interacting individuals are more relevant behavioral units for these social species. To fill key data gaps on group responses of social delphinids that are exposed to navy MFAS in large numbers, we describe novel approaches for the coordinated collection and integrated analysis of multiple remotely-sensed datasets during CEEs. This involves real-time coordination of a sonar source, shore-based group tracking, aerial photogrammetry to measure fine-scale movements and passive acoustics to quantify vocal activity. Using an example CEE involving long-beaked common dolphins (*Delphinus delphis bairdii*), we demonstrate how resultant quantitative metrics can be used to estimate behavioral changes and noise exposure-response relationships.

1. Introduction

Marine mammal species rely critically on sound production and reception for vital life functions, including reproduction, foraging, predator avoidance, and spatial orientation (Tyack, 2008; Southall, 2017). The potential for human noise to interfere with such functions was recognized half a century ago (Payne and Webb, 1971) and has been addressed with increasing resolution and detail in the decades since (e.g., National Research Council, 1994, 2003; Simmonds et al., 2014; National Academies of Sciences, 2017; Southall et al., 2019a). These issues have also been the subject of increasing interest and awareness within national and international regulatory bodies (e.g. Chou et al., 2021). There are valid concerns about both long-term consequences of increasing ocean noise levels from aggregate and chronically-present human noise sources, as well as discrete effects from intense, acute noise events.

Recent concern has focused on mid-frequency active sonars (MFAS, 3–8 kHz) that are used for submarine detection in navy training exercises and warfare (Filadelfo et al., 2009), because of the association of their use with a number of atypical mass stranding events of deep-diving

☆ Funding: This work was supported by the U.S. Navy's Office of Naval Research (Award Numbers N000141713132, N0001418IP-00021, N000141712887, N000141912572). The funding source had no involvement in study design, the collection/analysis/interpretation of data, writing of the manuscript or the decision to submit for publication.

* Corresponding author at: Southall Environmental Associates, Inc., 9099 Soquel Drive, Aptos, CA 95003, USA.
E-mail address: john.durban@sea-inc.net (J.W. Durban).

https://doi.org/10.1016/j.marpolbul.2021.113194
Received 5 May 2021; Received in revised form 21 November 2021; Accepted 23 November 2021
Available online 10 December 2021

whales (e.g. Parsons, 2017). Consequently, considerable research has focused on characterizing behavioral responses of cetaceans to both simulated and actual naval sonar sources (e.g. Tyack et al., 2011; DeRuiter et al., 2013; Goldbogen et al., 2013; Moretti et al., 2014; Falcone et al., 2017; Southall et al., 2019b; Wensveen et al., 2019; Joyce et al., 2020), with inferential power improved by the use of controlled exposure experiments (CEE; Southall et al., 2016; Harris et al., 2018).

These behavioral response studies have made major progress in identifying and characterizing responses to sonar exposure for several large whale and medium-sized cetacean species, particularly through the use of high-resolution and multi-sensor tags (Johnson and Tyack, 2003). However, efforts to deploy such tags on free-ranging smaller delphinids have been generally unsuccessful due to the tag size relative to their smaller bodies and increased drag resulting from their high swimming speeds. Furthermore, because dolphin species typically occur in groups, whose members interact in their response to external stimuli (Visser et al., 2014, 2016), the group is likely the more relevant unit for behavioral analysis. Consequently, fundamentally different methods are required to understand how these social and fast-moving species behave and respond to sonar. This represents a significant data gap, as dolphin species are often the most numerous cetaceans in navy operational areas that experience regular MFAS and other sonar events. As such, direct measurements of behavioral responses to exposure are required to understand, predict and mitigate the potential effects of sonar operations on these abundant species. This has direct relevance for navies to comply with legal requirements and for regulatory agencies to implement the statutes for these protected species.

To date, potential responses of small delphinids to sonar have been estimated in contexts that are challenging to apply in quantitative and predictive functions to inform such regulatory assessments. Laboratory observations (e.g. Houser et al., 2013) have provided direct measurements of exposure and response in known conditions, but with exposure contexts completely different than those experienced by free-ranging animals. Limited anecdotal observations of behavioral changes in response to sonar have been made for some free-ranging delphinids (e.g. Henderson et al., 2014), but in uncontrolled contexts which lack calibrated measurements of exposure levels and duration, and provide a largely subjective interpretation of general behaviour. Here we describe a novel approach for collecting quantitative data on several aspects of dolphin group responses using a suite of remote sensing methods during CEEs employing sonar. This controlled experimental approach involves real-time coordination of a simulated navy sonar source, shore-based theodolite tracking from an elevated vantage point to count and quantify movements of sub-groups within the larger group, aerial photogrammetry to measure finer scale movements of a focal sub-group and passive acoustic recordings to quantify group vocal activity. Using an example CEE involving long-beaked common dolphins (*Delphinus delphis bairdii*) near Santa Catalina Island, off southern California (U.S.A.), we demonstrate how the resultant quantitative metrics from each of these complimentary methods can be integrated by statistical inference to identify behavioral changes and estimate exposure-response relationships (Harris et al., 2018).

2. Methods

2.1. Experimental sound source and noise exposure sequences

Similar to previous CEEs with tagged cetaceans in the same region (Southall et al., 2012, 2019b), we used an experimental MFAS source (3–4 kHz) consisting of vertical line array (VLA) of active elements. This VLA has 15 individual transducer elements, each driven by an individual 800 W class D power amplifier. The experimental sound source was deployed to a depth of 25 m from a small (7.4-m) rigid-hull inflatable boat (RHIB). At the start of each CEE, the sound source was positioned at a range of between 1 and 3 km from the dolphins, determined from in situ propagation model estimates such that the received level for a focal experimental group reached sound pressure levels (SPL) from 120 to a maximum of 160 dB re 1 μPa (root-mean-squared); hereafter given as RL. Signals had a nominal source level of 212 dB SPL at 1 m, which is substantially below the unclassified level of 235 dB SPL of navy vessel-based MFAS systems but quite similar to the unclassified level of 215 dB SPL of helicopter-dipping MFAS. Signals consisted of a 1.6 s total duration sequence of three tonal and frequency-modulated elements from 3.5–4 kHz repeated on a 25 s duty cycle (see Southall et al., 2012). No experimental ramp-up of source levels was used for this project - all exposures occurred at a constant level to simulate realistic navy sonar operations.

The CEEs were comprised of three discrete phases: pre-exposure (baseline), exposure using intermittent MFAS signals as described above, and post-exposure. Each phase was 10 min in duration, with the exposure phase comprising 24 total pings, provided that no permit-mandated shut-downs occurred for animals occurring too close (within 200 m) to the active sound source. This was designed such that the entire CEE could be monitored during a single octocopter drone flight (see *2.3*), but it is also consistent with typical durations of navy training operations, particularly MFAS transmissions from arrays dipped into the water from a helicopter platform.[1] The timing of each CEE was coordinated with the collection of aerial images by the octocopter, with the start of the first phase being triggered in real time by the first aerial image collected of the focal group (or subgroup if the overall group was large and dispersed; see *2.2*).

2.2. Shore-based group selection and observations

Shore-based observations were made from elevated locations (~70 m) that enabled a broad overview of the research area (up to 20 km from shore) and an elevated view of the typically large aggregations of several hundred dolphins. Focal group selection prior to the start of experiments was based on location in the research area and sightability (i.e., expected to remain within view over the course of the experiment, and without other vessels nearby), group size and geometry metrics (very large groups, >750 individuals, or very scattered individuals were found too large or ephemeral to track consistently) and behavioral metrics (very fast movement, long dive times precluded consistent tracking). Mixed-species groups were excluded to enable comparison across experiments. Groups could be composed of one or several sub-groups, and corroboration with boat-based observations indicated that reliable shore-based tracking of group structure and spacing could be performed for groups up to 7 km from shore. A sub-group was defined following Visser et al. (2014), as all individuals in closer proximity to each other than to other individuals in the area. The group was defined similarly, but using sub-groups as the unit of observation, with groups consisting of all sub-groups in closer proximity to each other than to other (sub) groups in the area. Thus, observed from above, (sub-)groups were visible as distinct clusters of individuals. This operational definition of (sub-) groups allowed for the tracking of the same discernable unit throughout an experiment, and enabled quantitative recording of changes in cohesion metrics (i.e. group size, number of sub-groups, distance between individuals).

Observations consisted of two components: the recording of 1) group behaviour (focal follow observations) and 2) location of a sub-set of individuals in the group (theodolite-based tracking). Focal follows involved recording the group size and the number of sub-groups at 2-min intervals (Visser et al., 2014), using strong magnification binoculars or a binocular scope. Longer-term, remote tracking of one and the same focal individual in larger groups of often fast-moving and diving individuals is not possible. We therefore designed a tracking routine that enabled the construction of multiple short-term tracks, together

[1] https://www.hstteis.com/Documents/2018-Hawaii-Southern-California-Training-and-Testing-Final-EIS-OEIS/Final-EIS-OEIS

identifying the group track. Location-tracking was conducted by random selection of a small subset of tightly grouped individuals in the focal group, which was then tracked for as long as the observer was certain that the same individuals were in view. If the focal animals were lost, a new small focal unit was selected for tracking. This procedure was repeated until the end of the experiment. Tracking was conducted at as high a sampling rate as possible, aiming for 1 sample per surfacing and thus near-continuous tracking of the surface location. Location was recorded using a theodolite (Sokkia DTM5) linked to a computer running localization and mapping software (VADAR, Kniest, 2012). Focal follow observations always included the full focal group, including all-sub groups (*G;* see *2.9*). If the group extended beyond the sub-group imaged by the octocopter, the shore-based theodolite tracking focused on detailed movement of a separate sub-group.

2.3. Aerial images

Aerial images of a focal group, or sub-group, of dolphins (Fig. 1) were collected using a remotely controlled octocopter drone (APO-42, Aerial Imaging Solutions), which was launched, piloted and retrieved by hand from the bow of a 20 m charter dive boat. The octocopter used the same flight control and camera systems described by Durban et al. (2015). A micro 4/3 digital camera (Olympus *E*-PM2) and a 25 mm lens (Olympus M. Zuiko F1.8) were mounted in a powered gimbal to collect vertical images from directly above the dolphins from known altitudes of approximately 60 m. This altitude was chosen to achieve a compromise of flying sufficiently low to provide a water-level pixel resolution of <1.8 cm but also high enough to cover a relatively large image footprint on the water to encompass all or most of the focal subgroup (footprint of 42×31 m $= 1302$ m^2 at an altitude of 60 m). A laser altimeter (Dawson et al., 2017) mounted on the camera gimbal recorded precise (<0.1% error) altitude throughout each flight.

A maximum flight endurance of 35 min enabled octocopter operations to span all three phases of the CEE, during which the pilot-boat maintained a consistent contact distance typically between 300 and 500 m from the focal dolphins. The pilot was guided by a live video transmission that was monitored on a portable ground unit in real-time by a co-pilot to facilitate targeting of the same focal dolphins in the frame for as long as possible during the CEE. Once contact with the group had been established, the pilot remotely triggered the camera to record 16MP digital still photographs (Olympus Raw Format) at one-second intervals for the entire time that the dolphins were visible in the camera's footprint. The two-dimensional location of the octocopter was recorded by a 21-channel onboard GPS unit and the magnetic heading was measured by a microelectromechanical systems compass. All sensor measurements were linked to the time of each image to enable subsequent photogrammetry calculations (see *2.8*).

2.4. Passive acoustic recordings

Continuous passive acoustic monitoring (PAM) of dolphin vocalizations was conducted throughout each CEE using drifting, remote-deployed passive acoustic recorders (SNAP model 2.0; Loggerhead Instruments, Sarasota, FL) with individually-calibrated HTI-96 hydrophones (sensitivity −170 dB re 1 μPa/V, flat frequency response from 0.002–30 kHz). Recorders were deployed in close proximity to focal groups and suspended to a depth of 10 m under free-floating shock-mounted surface floats with Global Positional System (GPS) tracking devices (Trace, SPOT LLC, Chantilly, VA). The relative short deployment times and the high capacity (256 GB) flash memory allowed for continuous passive acoustic recording at a 48 kHz sampling rate and 16-bit resolution, and rapid offloading of data after each CEE. Up to three separate PAM recorders were strategically placed and recovered from a single small (~6 m) RHIB, with a goal of placing one PAM recorder within 500 m of the predicted track of the dolphins during each CEE phase (see Supplement 1). The location of these deployments was determined in real time based on the behaviour and direction of travel of the focal group. Deployments were coordinated with the other experimental components by VHF radio instructions from a coordinator who had an overview from the higher vantage point (elevation ~5.5 m) flybridge of the drone pilot-boat. To mitigate against disturbing and/or attracting dolphins, the RHIB operated at slow speed (<15 km/h) following positional instructions from the coordinator, who worked alongside visual observers on the same elevated flybridge to monitor any behavioral change of the focal dolphins relative to the RHIB's movement.

2.5. Field assessment and adaptive decision-making

To assess the efficacy of the experimental configuration, we designed a set of custom R scripts (R version 3.6.1, The R Foundation for Statistical Computing) to import, process, and visualize the spatial positioning and temporal tracks of each experimental component. This made use of all experimental components which had an associated GPS sensor, including the RHIB with the MFAS source, the second RHIB deploying the PAM recorders and location of the octocopter over the focal dolphins. For the shore observations, the location of animal sightings in geographic coordinate space was calculated from theodolite readings (Kniest et al. 2012). Using the *Leaflet* package (Cheng et al., 2019), we created a set of interactive maps that incorporated the track of all the

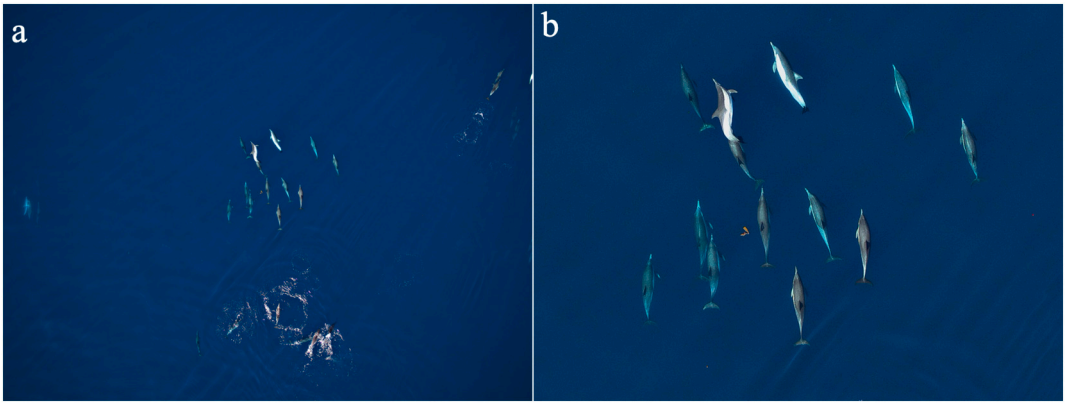

Fig. 1. a) Aerial image of long-beaked common dolphins collected using a vertically-gimballed camera mounted on a remote-controlled octocopter drone. The uncropped frame (a) shows a focal sub-group with other peripheral sub-groups taken from an altitude of 60.6 m (uncropped image footprint = 41.9 m × 31.5 m). The cropped zoom of the sub-group (b) shows the resolution available for photogrammetry measurements. Camera sensor dimensions, lens focal length, laser altitude, GPS coordinates and compass readings were combined to project pixel coordinates to geographic scale to produce sub-group movement tracks over time.

various components, which allowed a comprehensive assessment of the aggregate design. Using the *Shiny* package (Chang et al., 2019), we created an interactive animation application that showed the components' relative positioning in space and time (Supplement 1), which allowed a finer resolution examination of component positioning as the experiment progressed. These tools allowed us to critically assess the placement of each component and adaptively manage subsequent CEEs.

2.6. Estimating received levels

Using the known location of the MFAS source, we modeled the RL for focal group locations, taken as the GPS position of the octocopter, at the time of six pings spaced at approximately 2-min intervals throughout the 10-min exposure. Modeled RLs at the positions of acoustic recorders were compared to RLs measured by the recorders at their known depths and locations to evaluate modeling error. Deviations were generally within 3 dB and never exceeded 6 dB. Modeled RLs were used for these corresponding six pings as well for each closest ping before and after (for example the modeled RL for ping 5 was also used for pings 4 and 6), given that portions of focal groups could be reasonably expected to be at or near that location within 25 s. We estimated RLs for intervening pings using linear interpolation from modeled values. To determine RLs at 5-s intervals between pings, we used calibrated measurements of reverberation within the 3–5 kHz band made for the same MFAS source used in similar areas (Guan et al., 2017); time-specific differences in band levels from the direct path signals during transmissions were subtracted from on-ping levels to determine levels at intervening 5-s intervals. Ambient noise in the pre- and post-exposure phases was estimated at 81 dB RL based on measurements by Guan et al. (2017); this value was also used when reverberation from modeled or interpolated RL indicated lower values.

2.7. Passive acoustic analysis

To evaluate which PAM recorder was closest to the focal group given their frequently unpredictable course, the relative proximity of the hydrophone to the animals was determined *post-hoc* during each of the three CEE phases. At the onset of the each of the 10-minute experimental phases, the distance between the hydrophone location (based on its recorded GPS location) and the location of the focal group (determined by the GPS position of the octocopter) was calculated using a customized script in R (R version 3.6.1, The R Foundation for Statistical Computing). Recordings obtained from the hydrophone that was closest to the target group at the beginning of each of the CEE phase were selected for further analysis.

Standardized 5-second spectrograms were randomly generated every 30 s during the pre, exposure, and post exposure phases using Matlab 2016b (Mathworks, Natick, MA, USA; fast Fourier transform size 1024 samples, Hamming window, 50% overlap). This resulted in 20 5-second spectrograms for each of the three experimental phases (60 × 5-second windows in total). Each 5-second spectrogram was exported as an image file to enable standardized visual inspection by expert observers. To quantify group vocal activity, dolphin whistles were visually traced in a photo editing program and counted by three independent observers. Whistles were defined as a tonal, frequency-modulated signal greater than 0.1 s in duration (Caldwell and Caldwell, 1965). For the common dolphins in our example CEE (see *3* below), these whistles were typically in the 5–15 kHz frequency range (Oswald et al., 2021) and were clearly visible within the frequency range of the hydrophones (0.002–30 kHz). Previous studies have provided strong validation for the reliability of visual detection of odontocete whistles (Sayigh et al., 2007). The three sets of whistle counts for each of the 5 s periods were averaged (average = *W*, see 2.9), as a high degree of reliability was found between observers. The average intraclass correlation coefficient was 0.889 with a 95% confidence interval from 0.80 to 0.94 ($F[59,27.9] = 33, p < 0.001$), as estimated using the *irr* package in R (Gamer et al., 2019).

2.8. Spatially-explicit aerial photogrammetry

Starting with the first image within each flight that contained dolphins, each individual was located within the image frame using a custom workflow developed in the open-source image analysis program ImageJ (Abràmoff et al., 2004). The locations and orientations of individuals were recorded in pixel coordinates by drawing lines connecting the tip of the rostrum (beak) with the notch of the tail fluke. Individuals were then tracked from frame to frame by moving the lines from the previous image onto the rostrum tips and fluke notches of the same individuals in the subsequent image. Individuals were identified in sequential frames based on position and orientation relative to other dolphins within the frame as well as body size and markings. If there was any question as to whether a dolphin represented the same individual in sequential frames a new line was drawn, which started a new sequence of individual measurements with a new unique identification code.

Individuals were subsequently geolocated in geographic coordinate space by combining the pixel coordinates recorded in ImageJ with telemetry sensor information through a sequence of calculations conducted in R (R version 3.6.1, The R Foundation for Statistical Computing). The linear distances of rostrum tip coordinates from the center of the frame were calculated by multiplying the distance from the center of the frame in pixel dimensions by the Ground Sampling Distance (GSD), which denotes the width in meters at ground level represented by a single pixel (Baker, 1960). GSD was calculated using the following formula, with parameters of camera altitude measured by the laser altimeter on the camera gimbal, lens focal length (0.025 m), and sensor width in pixels (4608 pixels) and in meters (0.0173 m):

$$\mathrm{GSD} = \frac{\text{Altitude (m)}}{\text{Focal Length (m)}} * \frac{\text{Sensor Width (m)}}{\text{Sensor Width (pixels)}}$$

True bearings from the center of the frame to the rostrum tip coordinates of each individual were subsequently calculated based on: 1) relative bearings within each image frame, 2) the magnetic heading of the octocopter, and 3) local magnetic declination corresponding to the location and time stamp of each frame (Kelley and Richards, 2019). Using GSD, true bearing, and the GPS coordinates of the octocopter (assumed to represent center of the frame), the geographic coordinates of each individual rostrum tip were calculated using the *destPoint* function in the R package *geosphere* (Hijmans, 2019). Image distortion and resultant measurement error was assumed negligible. This was minimized due to our use of a powered gimbal to capture vertical images perpendicular to the water surface and a "normal" lens and sensor combination to ensure that the full field of view was flat for measurements (see Durban et al., 2015). Furthermore, the laser altimeter was mounted on the powered gimbal to measure vertical altitude even if the drone was tilted on one or both axes.

In the example CEE presented here, we selected a single dolphin at a time to estimate movement parameters for the group. The dolphin located closest to the center of the frame was selected as the focal dolphin, and a sequence of the geographic coordinates of its rostrum tip across frames was generated until unequivocal tracking of this individual was not possible. At this point, a new focal dolphin was selected by virtue of being closest to the center of the frame and a new sequence of coordinates was generated. A group track was therefore formed by combining the continuous sequences of coordinates for consecutive focal dolphins. This track was then used to statistically describe the group's movement throughout the CEE by fitting the continuous-time correlated random walk movement model (CTCRW, Johnson et al., 2008) to the two-dimensional location coordinates (latitude and longitude), and the time difference between adjacent locations. In the CTCRW model the movement process is governed by two free parameters: β describes directional persistence and σ controls overall variability in velocity. Instantaneous speed can be calculated from the modeled track (Johnson et al., 2008). We adopted a Bayesian formulation of the

CTCWR model, which provided an intuitive framework for hierarchically modeling these free parameters to assess behavioral changes (see 2.9; Michelot and Blackwell, 2019).

2.9. Statistical inference about behavioral changes

To demonstrate the value of monitoring group responses from a suite of complementary remote sensing methods, we performed similar analyses of response variables measured by each of the observational approaches of aerial photogrammetry, passive acoustics and shore-based tracking. To detect changes in response variables we assumed an underlying hidden Markov model (HMM; MacDonald and Zucchini, 1997) as a proxy for the group's behavioral state process (DeRuiter et al., 2017), and used Markov Chain Monte Carlo (MCMC) to carry out Bayesian inference about state changes (Scott, 2002). Specifically, the distribution of each response variable W (number of whistles) and G (number of sub-groups), and the set of movement response variables β and σ, was modeled by an independent HMM with two states:

$$log(Response_t) = \lambda_0 + \lambda_1 Z_t$$

where at each time step t the hidden state took values of $Z_t = 0$ to identify one state with a baseline response level λ_0, or $Z_t = 1$ to identify an "enhanced" state with λ_1 representing the enhancement to the quantitative value of the response variable. A flat uniform (−30,30) prior distribution was used for λ_0 in each response model and a uniform (0,30) prior distribution was adopted for λ_1 to constrain it to be positive. Therefore, the addition of λ_1 described more whistles and more subgroups (reduced group cohesion) in the enhanced state for these response variables. For the movement parameters, enhanced values for β induced less directional persistence and higher values for σ described more variation in velocity, which in combination described less consistent movement in the enhanced state. We did not specify when or if state changes occurred, but rather this was inferred by estimating the value of the latent state indicators, Z. The probability of being in the enhanced state was modeled by terms describing autocorrelation persistence, γ_1, and an effect of sonar received level, γ_2:

$$\text{logit}\{p(Z_t = 1)\} = \gamma_0 + \gamma_1 Z_{t-1} + \gamma_2 RL_t$$

where logit(p) = log{p/(1 − p)}. The utility of including the intercept, γ_0, was that the effects on this mean has prior distributions centered on zero, and we could simply estimate the posterior probability of a sonar effect on the enhanced response level by monitoring the proportion of MCMC iterations where γ_2 was >0. Uniform (-30,30) prior distributions were set on each of γ_0, γ_1 *and* γ_2.

To complete the specification of Bayesian full probability models, the response variables W and G were both assumed to be Poisson distributed counts of whistles and subgroups, respectively, and separate HMMs were fit to each. Movement parameters β and σ were derived from the

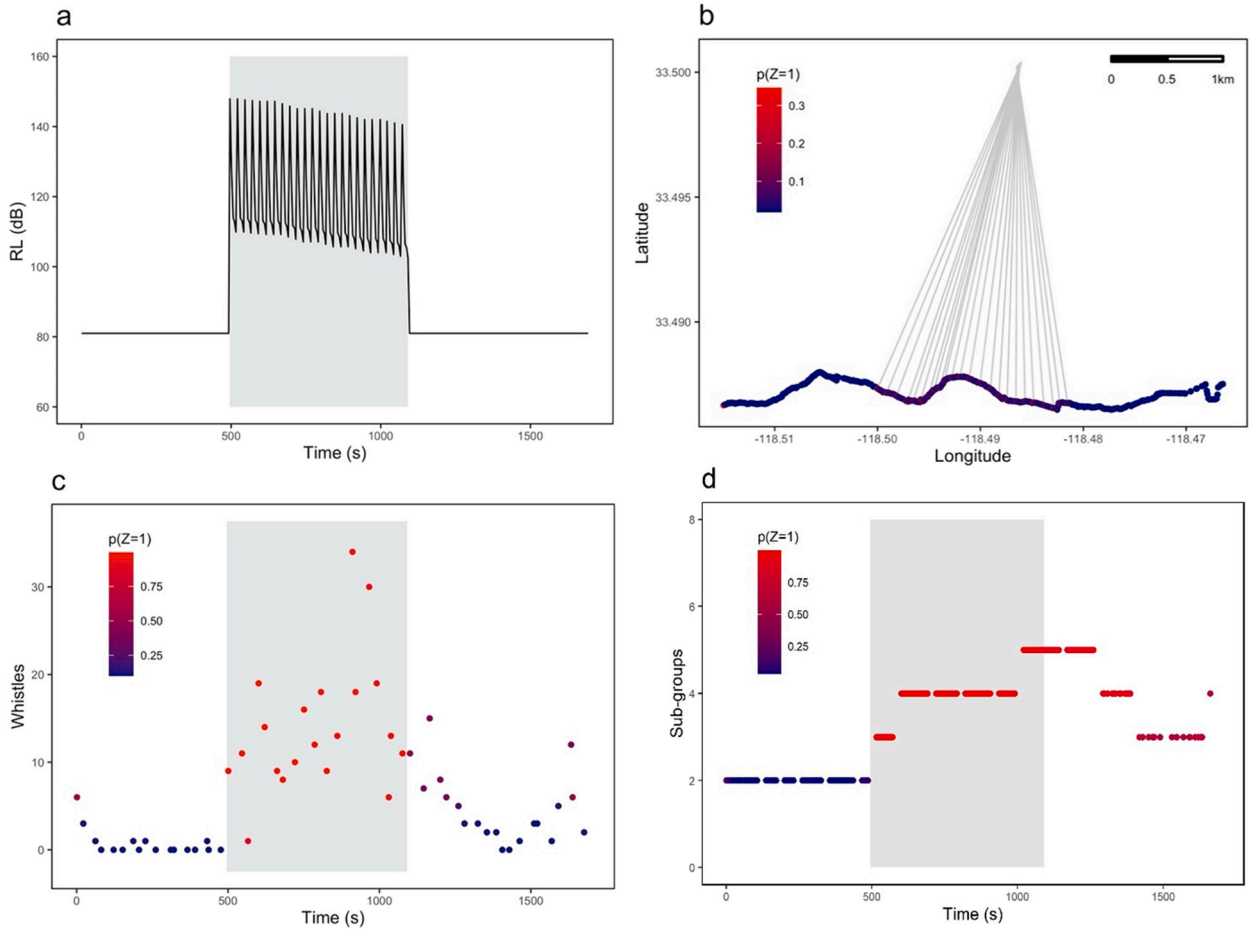

Fig. 2. a) The sound received level (RL) estimated at the location of the focal dolphin sub-group during a controlled exposure experiment with three phases: pre-exposure, exposure to 24 sonar pings spanning 10-minutes (gray shading) and post-exposure. b) Location track of the focal dolphin subgroup estimated from drone photogrammetry with the time of sonar pings and the bearing to the sonar source (gray lines); group track runs west to east (left to right). c) Counts of the number of whistles from the dolphin group recorded by passive acoustic monitoring. d) Counts from a shore-based overview of the number of sub-groups comprising the overall group. All are presented at a 5-second resolution; for b-d the observed data are color coded for the probability of an enhanced state of response $p(Z = 1)$ estimated from a hidden Markov model fit to estimated parameters of a movement model (b) and count data (c-d).

normally distributed location data in the Bayesian formulation of the CTCRW model (Michelot and Blackwell, 2019). The CTCRW and an HMM model for movement were fit simultaneously with the same MCMC sampler, to propagate uncertainty about both movement parameters directly into a single HMM to make inference about state changes from the two parameters in combination. In each model, change in state was evaluated at the temporal resolution of 5-s blocks to match the 5-s resolution of RL levels, and aligned with the timing of the 5-s whistle counts, *W*. Whistle counts were only available in a randomized number of blocks, and otherwise were treated as unknown to be estimated during MCMC. The number of subgroups, *G*, was only recorded during periodic observations every 2 min, or when it was detected to have changed, and assumed constant across blocks between observations. However, *G* was treated as missing data 30 s before each change was noted, to introduce prior uncertainty about the precise timing of change (Fig. 2).

Bayesian formulations of CTCRW and HMM models were programmed in R (R version 3.6.1; The R Foundation for Statistical Computing) with the *nimble* package (de Valpine et al., 2020) used to estimate posterior distributions of model parameters using MCMC. Inference was based on 100,000 MCMC samples following a burn-in of 100,000, with chain convergence determined by visual inspection of three MCMC chains and corroborated by convergence diagnostics (Brooks and Gelman, 1998). To visualize an exposure-response relationship with RL for each model fit, the same 100,000 iterations were used sample from the stationary posterior distribution of model parameters to evaluate the predictive probability, p^e, of each response being in the enhanced state for each of $i = 140$ equally-spaced theoretical RLs from 60 to 200 dB:

$$p^e{}_i = exp(\gamma_0 + \gamma_1 + \gamma_2 RL_i)/\{1 + exp(\gamma_0 + \gamma_1 + \gamma_2 RL_i)\}$$

2.10. An example experiment

We conducted a CEE with a group of long-beaked common dolphins on June 21st 2018 off the north side of Santa Catalina Island (33.49^{0}N; 118.50^{0}W; Supplement 1), approximately 35 km southwest of the Port of Los Angeles-Long Beach. The group was initially sighted by the shore-based observation team, which directed the three boat platforms into position. The pre-exposure phase began at 10:49:40 am local time (Pacific Daylight Time) in calm weather, flat surface water conditions and bright overcast skies for observations.

The shore-based observers estimated the size of the entire group as approximately 300 individuals, comprised of between two and five subgroups that were dynamic in fission and fusion over the course of the CEE (Fig. 2). The focal sub-group for photogrammetry monitoring contained approximately 20 individuals and was monitored by an octocopter flight lasting 34 min, with 1614 images taken spanning a total of 2041 s, covering all three 10-minute phases of the CEE. The sub-group track from this flight was segmented into 37 focal animal sequences ranging in length from 2 to 186 s (median = 38 s). Three PAM recorders were deployed at times 192 s prior to the pre-exposure phase, 280 s prior to the exposure phase and 36 s into exposure, respectively, at an estimated distance of 0.70–0.76 km to the focal sub-group at the time of deployment. Dolphin whistles were recorded on the first two of these recorders, with the first recorder being used for the pre-exposure phase and the second for the exposure and post-exposure phases. A median of 4 whistles were counted per 5-second time block, with significant variability from zero to 36 whistles. The MFAS source was positioned 2.9 km away from the focal subgroup at the start of the exposure phase and 3.3 km away at the end. RL at the focal subgroup was estimated to range from 147.9 dB at the start to 102.5 dB at the end of the exposure phase (Fig. 2).

The probability of the focal group being in the model-defined "enhanced" state differed between the response variables in each HMM. The probability was highest for the number of whistles and sub-groups: transformation of the intercept (γ^0, Table 1) showed an average $p(Z_t = 1)$ of 0.41 and 0.56 for the number of whistles (*W*) and sub-groups (*G*), respectively, compared to only 0.03 for the movement parameters β and σ in combination. This movement effect was also subtle, resulting in average speed of the focal sub-group per 5-second block dropping from 12.8 km/h when $p(Z_t = 0)$ to 10.2 km/h when $p(Z_t = 1)$, indicating power to detect small changes. Notably, the probability of transitioning to the enhanced state increased during the 10-minute exposure phase of the experiment for all response variables (Fig. 2). As such, the probability of being in the enhanced state was estimated to have a significant positive relationship with sonar RL for all three response variables (Table 1), with $p(\gamma_2 > 0)$ of 0.98, 1.00 and 0.99 for movement, whistle counts, and sub-groups counts, respectively. Posterior estimates of the persistence parameter (γ_1, Table 1) indicated that the enhanced state effect of reduced social cohesion persisted for longest, with relatively high sub-group counts continuing after the exposure phase and throughout the post-exposure phase (Fig. 2). The persistence parameter was lower for whistle counts, with an enhanced effect on acoustic activity persisting throughout the exposure phase but becoming less likely post-exposure. The persistence estimate was lowest for the movement parameters, indicating that transitions to the less directional enhanced state were of short duration and almost entirely within the exposure phase of the experiment (Fig. 2). Varying parameter estimates, and their precision, were reflected in the variable shape and uncertainty of exposure-response relationships (Fig. 3). In each case, the probability of a response (transitioning to the enhanced state) was positively related to increasing RL, but the magnitude of this response probability was notably lower for the movement parameters across this specific CEE.

3. Discussion

Detecting and characterizing behavioral responses of cetaceans to sound exposure is challenged by context-dependent differences in responses, including the importance of species sensitivity, individual behavioral state and the physical range to the sound source (e.g. Ellison et al., 2018; Southall et al., 2016, 2019b; Pirotta et al., 2021). This strongly suggests that measurements of response should be made in as realistic exposure scenarios as possible with experiments designed to provide controlled replicates across exposure contexts (Southall et al., 2016). Our novel and integrated experimental design helps to address the specific challenges that have constrained realistic behavioral response studies on abundant delphinid species, which typically occur and respond in groups. Our approach builds on previous CEEs that have used tags on individuals from larger cetacean species to quantify behavioral responses to navy sonar exposure (see Southall et al., 2016, 2019b). Specifically, to enable the monitoring of group responses of small dolphin species that are not amenable to tagging, we adopted a suite of remote observational methods coordinated in real-time with a sonar source during CEEs. This coordination is challenging, but in combination these methods are powerful for quantifying changes in behaviour.

We demonstrate that these observational methods are complimentary by differing in the aspect and scale of group responses measured. Movement modeling of aerial photogrammetry data enables subtle movement responses to be detected. Non-invasive drones capable of stable flight can track high-speed dolphins and collect high-resolution imagery, allowing movement models to be fit to precise measurements of the positioning of individuals in focal sub-groups. The high vantage view offered by shore-based observations allows for consistent tracking of large groups over a wide area, thus providing cohesion and movement data to evaluate group structure at a larger scale. The use of passive acoustic recording allows additional insight into non-visual responses, which are likely important for highly social species that readily use acoustic cues for social communication. The application of each of these methods on their own is not novel, but we provide the first demonstration of how their coordination in the field can allow diversity in

Table 1
Parameter estimates from fitting a two-state hidden Markov model (HMM) hierarchically to describe variability in directional persistence (β) and variation in velocity (σ) parameters from a continuous-time correlated random walk movement model (Johnson et al., 2008) fit to drone-derived location tracks of a group of long-beaked common dolphins. Also shown are parameters for similar two-state HMMs fit separately to dolphin group whistle counts (*W*) from passive acoustic monitoring and the number of sub-groups (*G*) counted from a shore-based overlook. Parameters are shown for two components of the model describing 1) the baseline and enhanced level of each response variable, transformed from log scale, and 2) the probability of an enhanced state ($Z = 1$) on the logit scale. Posterior estimates are shown as means (standard deviation) of 100,000 Markov chain Monte Carlo iterations implemented in R with package NIMBLE (de Valpine et al., 2020).

	Response level		$\text{logit}\{p(Z_t = 1)\}$		
Variable	$\exp(\lambda_0)$ Base level	$\exp(\lambda_1)$ Enhancement	γ_0 Intercept	γ_1 Persistence	γ_2 Sonar effect
β, direction	0.48 (1.05)	7.93 (1.36)	−3.66 (0.39)	0.43 (1.02)	0.03 (0.01)
σ, velocity	0.00 (1.08)	7.45 (1.26)	−3.66 (0.39)	0.43 (1.02)	0.03 (0.01)
W, whistles	1.30 (1.27)	10.05 (1.25)	−0.36 (1.17)	2.31 (2.17)	0.14 (0.06)
G, subgroups	2.09 (1.10)	1.98 (1.10)	0.25 (1.39)	6.55 (0.89)	0.25 (0.10)

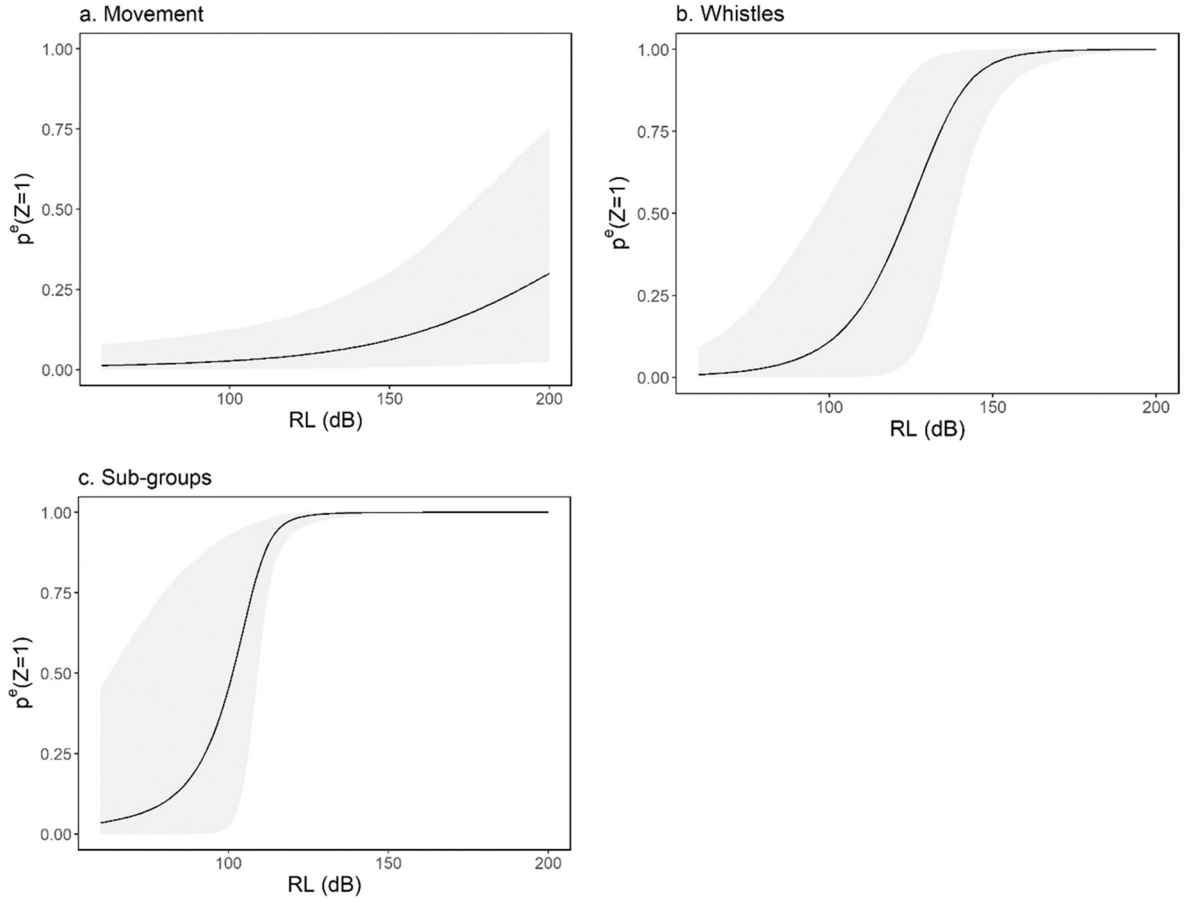

Fig. 3. Exposure-response curves of the probability, p^e, of an enhanced state of response ($Z = 1$) as a function of sonar received level (RL) for three types of responses: a) movement parameters describing directional persistence and variation in velocity of dolphin groups estimated from a continuous-time correlated random walk movement model (Johnson et al., 2008) fit to drone-derived group movement tracks; b) counts of whistles produced by dolphin groups in 5-second time blocks and c) counts of the number distinct sub-groups comprising the overall group. Dose responses to RLs ranging from = 60–200 dB were predicted from the fit of separate hidden Markov models using a Markov chain Monte Carlo sampler implemented in R with package *nimble* (de Valpine et al., 2020). Lines are posterior means, gray shading represents the 95% highest posterior density interval.

response behaviour to be captured to provide greater resolution for identifying responses.

We also demonstrate how these remote sensing and non-invasive methods can provide quantitative and objective metrics of behavioral change. Specifically, we fit HMM models to estimate latent state transitions and relationships with received sonar levels, which allows inference within a unifying framework of exposure-response relationships (Harris et al., 2018; Tyack and Thomas, 2019). This approach can be extended to describe variability in a range of response variables across a range of different exposure contexts as a greater number of experiments are conducted. The purpose of our example is to demonstrate how a suite of response variables from a variety of remote sensing methods can be integrated to identify behavioral responses, rather than providing a detailed characterization of these responses. We therefore adopt a relatively simple two-state HMM with a limited set of response variables. As additional response variables are considered, the HMM itself can be extended to provide more detailed inference, for example by using a multivariate HMM to parameterize state-switching between a larger number of latent states, which may be related to identifiable behavioral states (DeRuiter et al., 2017).

The approach presented here allows measurement of group level responses, but does not explicitly address if these are direct responses to the active sound source or responses to behavioral changes by other individuals or sub-groups. Nonetheless, we believe there are extensions to our methods that will provide greater resolution to examine for dependent responses that may occur through social facilitation (Zajonc, 1965). Our example photogrammetry tracking of group movement does not make use of available measurements of individual spacing, orientation and simultaneous tracking of different individuals, and response variables can be extended to model the dependent movement of multiple individuals (e.g. Scharf et al., 2016, 2018). Similarly, the spatial scale of the shore-based group tracking can be extended to model covariance in movement at the subgroup level as well as providing further empirical metrics such as sub-group spacing. Passive acoustic data can also be further utilized, for example to investigate finer scale vocal responses that may be undetected by the 5-second processing window. Such additional response variables will likely also be more sensitive for informing behavioral state transitions and might therefore narrow uncertainty about the exposure-response relationships.

In summary, the coordination and integration of remote sensing methods we describe enables objective and quantitative tracking of the fluid movement, social and acoustic behaviors of large groups of fast-moving dolphins, at fine-resolution as well as larger scale. These observational components can be effectively coordinated with a simulated navy sonar source in real time to maintain a controlled and known exposure context, which enables exposure-response relationships to be quantified. This represents a much-needed advance in our ability to understand behavioral responses of small delphinids to sonar exposure, which is essential given their propensity for frequent exposure due to their high abundance. Future developments should focus on building experimental sample sizes to describe species- and context-dependent differences in responses, including CEEs with real navy sonar sources. Efforts to achieve both these objectives are ongoing in subsequent phases of this study.

CRediT authorship contribution statement

J.W. Durban: Conceptualization, Methodology, Software, Validation, Formal analysis, Investigation, Resources, Data curation, Writing – original draft, Visualization, Supervision, Project administration, Funding acquisition. **B.L. Southall:** Conceptualization, Methodology, Validation, Formal analysis, Investigation, Resources, Data curation, Writing – review & editing, Supervision, Project administration, Funding acquisition. **J. Calambokidis:** Conceptualization, Methodology, Investigation, Resources, Supervision, Project administration, Funding acquisition. **C. Casey:** Methodology, Formal analysis, Investigation, Data curation, Writing – review & editing. **H. Fearnbach:** Methodology, Investigation, Data curation, Writing – review & editing. **T.W. Joyce:** Methodology, Software, Writing – review & editing. **J.A. Fahlbusch:** Investigation, Visualization, Writing – review & editing. **M.G. Oudejans:** Methodology, Investigation, Data curation. **S. Fregosi:** Methodology, Formal analysis, Investigation, Data curation, Writing – review & editing. **A.S. Friedlaender:** Conceptualization, Methodology, Investigation, Funding acquisition, Writing – review & editing. **N.M. Kellar:** Conceptualization, Methodology, Funding acquisition, Writing – review & editing. **F. Visser:** Conceptualization, Methodology, Validation, Formal analysis, Investigation, Resources, Data curation, Writing – review & editing, Supervision, Project administration, Funding acquisition.

Declaration of competing interest

The authors declare that they have no known competing financial interests or personal relationships that could have appeared to influence the work reported in this paper.

Acknowledgements

Funding for this work was provided by the U.S. Navy's Office of Naval Research (Award Numbers N000141713132, N0001418IP-00021, N000141712887, N000141912572), and we are particularly grateful to Mike Weise and Dana Belden. Octocopter flights over dolphins were authorized by NMFS permit 19091, and all animal close approaches for observations and CEEs were conducted under NMFS permit 19116. We would like to acknowledge the collaboration and support of Diane and Bernardo Alps, as well the M/V Magician and Captain Carl Mayhugh. We also very much appreciate the support and partnership with the University of Southern California's Wrigley Institute. This research was only possible as a result of the combined work by all the members of the dedicated and capable "Tagless BRS" field and analysis teams. We thank Jeff Seminoff and two anonymous reviewers for comments on earlier versions of this manuscript.

Appendix A. Supplement 1

Dynamic maps of the experimental components for the example CEE can be viewed at https://musculus.shinyapps.io/taglessshiny/.

References

Abràmoff, M.D., Magalhães, P.J., Ram, S.J., 2004. Image processing with ImageJ. Biophoton. Int. 11, 36–42.
Baker, W.H., 1960. In: Photogrammetry. The Ronald Press Company, New York, p. 199.
Brooks, S.P., Gelman, A., 1998. General methods for monitoring convergence of iterative simulations. J. Comput. Graph. Stat. 7, 434–455.
Caldwell, M.C., Caldwell, D.K., 1965. Individualized whistle contours in bottle-nosed dolphins (Tursiops truncatus). Nature 207, 434–435.
Chang, W., Cheng, J., Allaire, J.J., Xie, Y., McPherson, J., 2019. Shiny: Web Application Framework for R. R package version 1.4.0. https://CRAN.R-project.org/package=shiny.
Cheng, J., Karambelkar, B., Xie, Y., 2019. Leaflet: Create Interactive Web Maps with the JavaScript 'Leaflet' Library. R package version 2.0.3. https://CRAN.R-project.org/package=leaflet.
Chou, E., Southall, B.L., Robards, M., Rosenbaum, H.C., 2021. International policy, recommendations, actions and mitigation efforts of anthropogenic underwater noise. Ocean Coast. Manag. 202, 105427.
<collab>National Academies of Sciences, Engineering and Medicine N.A.S.collab, 2017. Approaches to understanding the cumulative effects of stressors on marine mammals. The National Academies Press, Washington, DC.
Dawson, S.M., Bowman, M.H., Leunissen, E., Sirguey, P., 2017. Inexpensive aerial photogrammetry for studies of whales and large marine animals. Front. Mar. Sci. 4, 366.
DeRuiter, S.L., Southall, B.L., Calambokidis, J., Zimmer, W.M., Sadykova, D., Falcone, E. A., Friedlaender, A.S., Joseph, J.E., Moretti, D., Schorr, G.S., Thomas, L., 2013. First direct measurements of behavioural responses by Cuvier's beaked whales to mid-frequency active sonar. Biol. Lett. 9, 20130223.
DeRuiter, S.L., Langrock, R., Skirbutas, T., Goldbogen, J.A., Calambokidis, J., Friedlaender, A.S., Southall, B.L., 2017. A multivariate mixed hidden Markov model for blue whale behaviour and responses to sound exposure. Ann. Appl. Stat. 11, 362–392.
Durban, J.W., Fearnbach, H., Barrett-Lennard, L.G., Perryman, W.L., Leroi, D.J., 2015. Photogrammetry of killer whales using a small hexacopter launched at sea. J. Unmanned Veh. Syst. 3, 131–135.
Ellison, W.T., Southall, B.L., Frankel, A.S., Vigness-Raposa, K., Clark, C.W., 2018. An acoustic scene perspective on spatial, temporal, and spectral. Aquat. Mamm. 44, 239–243.
Falcone, E.A., Schorr, G.S., Watwood, S.L., DeRuiter, S.L., Zerbini, A.N., Andrews, R.D., Morrissey, R.P., Moretti, D.J., 2017. Diving behaviour of Cuvier's beaked whales exposed to two types of military sonar. R. Soc. Open Sci. 4, 170629.
Filadelfo, R., Mintz, J., Michlovich, E., D'Amico, A., Tyack, P.L., 2009. Correlating military sonar use with beaked whale mass strandings: what do the historical data show? Aquat. Mamm. 34, 435–444.
Gamer, M., Lemon, J., Fellows, I., Singh, P., 2019. irr: Various coefficients of interrater reliability and agreement. R package version 0.84.1. https://CRAN.R-project.org/package=irr.
Goldbogen, J.A., Southall, B.L., DeRuiter, S.L., Calambokidis, J., Friedlaender, A.S., Hazen, E.L., Falcone, E.A., Schorr, G.S., Douglas, A., Moretti, D.J., Kyburg, C., 2013. Blue whales respond to simulated mid-frequency military sonar. Proc. R. Soc. B Biol. Sci. 280, 20130657.
Guan, S., Southall, B.L., Barlow, J., Vignola, J.F., Judge, J.A., Turo, D., 2017. Sonar interping noise field characterization during cetacean behavioral response studies off Southern California. Acoust. Phys. 63, 204–215.
Harris, C.M., Thomas, L., Falcone, E.A., Hildebrand, J., Houser, D., Kvadsheim, P.H., Lam, F.P.A., Miller, P.J., Moretti, D.J., Read, A.J., Slabbekoorn, H., 2018. Marine

mammals and sonar: dose-response studies, the risk-disturbance hypothesis and the role of exposure context. J. Appl. Ecol. 55, 396–404.
Henderson, E.E., Smith, M.H., Gassmann, M., Wiggins, S.M., Douglas, A.B., Hildebrand, J.A., 2014. Delphinid behavioral responses to incidental mid-frequency active sonar. J. Acoust. Soc. Am. 136, 2003–2014.
Hijmans, R.J., 2019. geosphere: Spherical Trigonometry. R package version 1.5-10.. https://CRAN.R-project.org/package=geosphere.
Houser, D.S., Martin, S.W., Finneran, J.J., 2013. Exposure amplitude and repetition affect bottlenose dolphin behavioral responses to simulated mid-frequency sonar signals. J. Exp. Mar. Biol. Ecol. 443, 123–133.
Johnson, M.P., Tyack, P.L., 2003. A digital acoustic recording tag for measuring the response of wild marine mammals to sound. IEEE J. Ocean. Eng. 28, 3–12.
Johnson, D.S., London, J.M., Lea, M.A., Durban, J.W., 2008. Continuous-time correlated random walk model for animal telemetry data. Ecology 89, 1208–1215.
Joyce, T.W., Durban, J.W., Claridge, D.E., Dunn, C.A., Hickmott, L.S., Fearnbach, H., Dolan, K., Moretti, D., 2020. Behavioral responses of satellite tracked Blainville's beaked whales (Mesoplodon densirostris) to midfrequency active sonar. Mar. Mamm. Sci. 36, 29–46.
Kelley, D., Richards, C., 2019. oce: Analysis of Oceanographic Data. R package version 1.1-1. https://CRAN.R-project.org/package=oce.
Kniest, E., 2012. Visual Detection and Ranging (VADAR), version 1.45.06. University of Newcastle, Callaghan, Australia.
MacDonald, I.L., Zucchini, W., 1997. Hidden Markov and other models for discrete-valued time series, 110. CRC Press.
Michelot, T., Blackwell, P.G., 2019. State-switching continuous-time correlated random walks. Methods Ecol. Evol. 10, 637–649.
Moretti, D., Thomas, L., Marques, T., Harwood, J., Dilley, A., Neales, B., Shaffer, J., McCarthy, E., New, L., Jarvis, S., Morrissey, R., 2014. A risk function for behavioral disruption of Blainville's beaked whales (Mesoplodon densirostris) from midfrequency active sonar. PLoS One 9, e85064.
National Research Council, 1994. Low-Frequency Sound in Marine Mammals: Current Knowledge and Research Needs. The National Academies Press, Washington, DC.
National Research Council, 2003. Ocean Noise and Marine Mammals. The National Academies Press, Washington, DC.
Oswald, J.N., Walmsley, S.F., Casey, C., Fregosi, S., Southall, B., Janik, V.M., 2021. Species information in whistle frequency modulation patterns of common dolphins. Philos. Trans. R. Soc. B 376, 20210046.
Parsons, E.C.M., 2017. Impacts of navy sonar on whales and dolphins: now beyond a smoking gun? Front. Mar. Sci. 4, 295.
Payne, R., Webb, D., 1971. Orientation by means of long-range acoustic signaling in baleen whales. Ann. N. Y. Acad. Sci. 188, 110–141.
Pirotta, E., Booth, C.G., Cade, D.E., Calambokidis, J., Costa, D.P., Fahlbusch, J.A., Friedlaender, A.S., Goldbogen, J.A., Harwood, J., Hazen, E.L., New, L., 2021. Context-dependent variability in the predicted daily energetic costs of disturbance for blue whales. Conserv. Physiol. 9, coaa137.
Sayigh, L.S., Esch, H.C., Wells, R.S., Janik, V.M., 2007. Facts about signature whistles of bottlenose dolphins, Tursiops truncatus. Anim. Behav. 74, 1631–1642.
Scharf, H.R., Hooten, M.B., Fosdick, B.K., Johnson, D.S., London, J.M., Durban, J.W., 2016. Dynamic social networks based on movement. Ann. Appl. Stat. 10, 2182–2202.
Scharf, H.R., Hooten, M.B., Johnson, D.S., Durban, J.W., 2018. Process convolution approaches for modeling interacting trajectories. Environmetrics 29, e2487.
Scott, S.L., 2002. Bayesian methods for hidden Markov models: recursive computing in the 21st century. J. Am. Stat. Assoc. 97, 337–351.
Simmonds, M.P., Dolman, S.J., Jasny, M., Parsons, E.C.M., Weilgart, L., Wright, A.J., Leaper, R., 2014. Marine noise pollution – increasing recognition but need for more practical action. J. Ocean Technol. 9, 71–90.
Southall, B.L., 2017. Noise. In: Würsig, B., Thiewesson, H. (Eds.), Encyclopedia of Marine Mammals, 3rd edition. Academic Press, New York, ISBN 9780128043271, pp. 699–707.
Southall, B.L., Moretti, D., Abraham, B., Calambokidis, J., Tyack, P.L., 2012. Marine mammal behavioral response studies in Southern California: advances in technology and experimental methods. Mar. Technol. Soc. J. 46, 48–59.
Southall, B.L., Nowacek, D.P., Miller, P.J.O., Tyack, P.L.T., 2016. Synthesis of experimental behavioral response studies using human sonar and marine mammals. Endanger. Species Res. 31, 291–313.
Southall, B.L., Finneran, J.J., Reichmuth, C., Nachtigall, P.E., Ketten, D.R., Bowles, A.E., Ellison, W.T., Nowacek, D.P., Tyack, P.L., 2019a. Marine mammal noise exposure criteria: updated scientific recommendations for residual hearing effects. Aquat. Mamm. 45, 125–232.
Southall, B.L., DeRuiter, S.L., Friedlaender, A., Stimpert, A.K., Goldbogen, J.A., Hazen, E., Casey, C., Fregosi, S., Cade, D.E., Allen, A.N., Harris, C.M., Schorr, G., Moretti, D., Guan, S., Calambokidis, J., 2019b. Behavioral responses of individual blue whales (Balaenoptera musculus) to midfrequency military sonar. J. Exp. Biol. 222, jeb190637.
Tyack, P.L., 2008. Implications for marine mammals of largescale changes in the marine acoustic environment. J. Mammal. 89, 549–558.
Tyack, P.L., Thomas, L., 2019. Using dose–response functions to improve calculations of the impact of anthropogenic noise. Aquat. Conserv. Mar. Freshwat. Ecosyst. 29, 242–253.
Tyack, P.L., Zimmer, W.M.X., Moretti, D., Southall, B.L., Claridge, D.E., Durban, J.W., Clark, C.W., D'Amico, A., DiMarzio, N., Jarvis, S., McCarthy, E., Morrissey, R., Ward, J., Boyd, I.L., 2011. Beaked whales respond to simulated and actual navy sonar. PLoS One 6, e17009.
de Valpine, P., Paciorek, C., Turek, D., Michaud, N., Anderson-Bergman, C., Obermeyer, F., Cortes, C.W., Rodrìguez, A., Lang, D.T., Paganin, S., 2020. Nimble: MCMC, Particle Filtering, and Programmable Hierarchical Modeling. R package version 0.9.1. https://CRAN.R-project.org/package=nimble.
Visser, F., Miller, P.J.O., Antunes, R.N., Oudejans, M.G., Mackenzie, M.L., Aoki, K., Lam, F.P.A., Kvadsheim, P.H., Huisman, J., Tyack, P.L., 2014. The social context of individual foraging behaviour in long-finned pilot whales (Globicephala melas). Behaviour 151, 1453–1477.
Visser, F., Curé, C., Kvadsheim, P.H., Lam, F.P.A., Tyack, P.L., Miller, P.J.O., 2016. Disturbance-specific social responses in long-finned pilot whales, Globicephala melas. Sci. Rep. 6, 28641.
Wensveen, P.J., Isojunno, S., Hansen, R.R., von Benda-Beckmann, A.M., Kleivane, L., van IJsselmuide, S., Lam, F.P.A., Kvadsheim, P.H., DeRuiter, S.L., Curé, C., Narazaki, T., 2019. Northern bottlenose whales in a pristine environment respond strongly to close and distant navy sonar signals. Proc. R. Soc. B 286, 20182592.
Zajonc, R.B., 1965. Social facilitation. Science 149, 269–274.